Color superconductivity in compact stellar hybrid configurations

Ignacio F. Ranea-Sandoval, Milva G. Orsaria, Sophia Han, Fridolin Weber, and William M. Spinella

Color superconductivity in compact stellar hybrid configurations

Ignacio F. Ranea-Sandoval*

*Grupo de Gravitación, Astrofísica y Cosmología,
Facultad de Ciencias Astronómicas y Geofísicas, Universidad Nacional de La Plata,
Paseo del Bosque S/N (1900), La Plata, Argentina and
CONICET, Godoy Cruz 2290, C1425FQB, Buenos Aires, Argentina*

Milva G. Orsaria†

*Grupo de Gravitación, Astrofísica y Cosmología,
Facultad de Ciencias Astronómicas y Geofísicas, Universidad Nacional de La Plata,
Paseo del Bosque S/N (1900), La Plata, Argentina
CONICET, Godoy Cruz 2290, C1425FQB, Buenos Aires, Argentina and
Department of Physics, San Diego State University,
5500 Campanile Drive, San Diego, California 92182*

Sophia Han‡

Department of Physics and Astronomy, University of Tennessee, Knoxville, TN 37996, USA

Fridolin Weber§

*Department of Physics, San Diego State University,
5500 Campanile Drive, San Diego, California 92182 and
Center for Astrophysics and Space Sciences,
University of California,
San Diego, La Jolla, CA 92093, USA*

William M. Spinella¶

*Computational Science Research Center and Department of Physics,
San Diego State University, 5500 Campanile Drive, San Diego, California 92182*

(Dated: November 21, 2017)

The discovery of pulsars PSR J1614–2230 and PSR J0348+0432 with masses of around $2M_\odot$ imposes strong constraints on the equations of state of cold, ultra-dense matter. If a phase transition from hadronic matter to quark matter were to occur in the inner cores of such massive neutron stars, the energetically favorable state of quark matter would be a color superconductor. In this study, we analyze the stability and maximum mass of such neutron stars. The hadronic phase is described by non-linear relativistic mean-field models, and the local Nambu-Jona Lasinio model is used to describe quark matter in the 2SC+s quark phase. The phase transition is treated as a Maxwell transition, assuming a sharp hadron-quark interface, and the "constant-sound-speed" (CSS) parametrization is employed to discuss the existence of stellar twin configurations. We find that massive neutron stars such as J1614-2230 and J0348+0432 can only exist on the connected stellar branch but not on the disconnected twin-star branch. The latter can only support stars with masses that are strictly below $2M_\odot$.

I. INTRODUCTION

Confronting neutron star observables, such as mass and radii [1, 2], with detailed theoretical calculations offers the intriguing possibility to probe matter at ultra-high densities and to put constraints on models for the equation of state (EoS) of such matter [3, 4]. For instance, the discovery of the massive pulsars PSR J1614-2230 [5] ($M = (1.928 \pm 0.017) M_\odot$ [6]) and PSR J0348+0432 ($M = (2.01 \pm 0.04) M_\odot$ [7]) have been used to rule out many theoretically proposed models for the EoS, which all fail to accommodate such high-mass neutron stars. Despite this success, the core composition of neutron stars is still largely unknown. In the most primitive conception, a neutron star is constituted from neutrons. At a more accurate representation, neutron stars, which are in chemical equilibrium, will contain neutrons and protons whose charge is balanced by leptons. At the densities in the interior of neutron stars, the neutron chemical potential is expected to exceed the mass (modified by interactions) of various members of the baryon octet, so that in addition to neutrons, protons and electrons, neutron stars are also expected to have populations of hyperons, which together with nucleons and leptons are in a charge-neutral equilibrium state. Lastly, the

———————

* iranea@fcaglp.unlp.edu.ar
† morsaria@fcaglp.unlp.edu.ar
‡ jhan18@utk.edu
§ fweber@mail.sdsu.edu
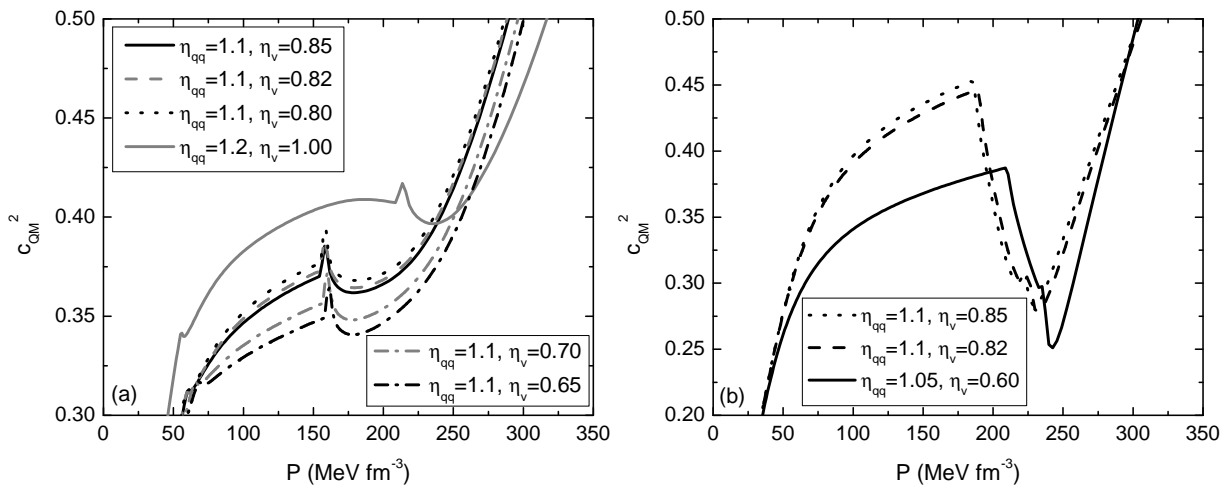¶ william.spinella@gmail.com

Figure 1. Square of the speed of sound, $c_{\rm QM}^2 \equiv dp/d\varepsilon$, for different 2SC+s quark EoSs with fixed strange quark mass $M_s^0 = 500$ MeV (a), 600 MeV (b). The model parameters used are the same as in Fig. 4 depicting the mass-radius relation of hybrid stars using NL3 for the hadronic EoS.

matter in the centers of neutron stars may become so highly compressed that a phase transition from hadronic matter to deconfined quark matter can occur in their cores [8–13]. Such neutron stars are referred to as quark-hybrid stars.

It has been argued that the ground state of quark matter consists of quark pairs which form a color superconductor [14, 15] where the attractive interaction between quarks emerges naturally through the exchange of gluons. As seen in the Bardeen-Cooper-Schrieffer theory of ordinary superconductivity, quarks with equal but opposite momenta at their respective Fermi surfaces form Cooper pairs to lower the energy of the system. Color superconductivity in the interiors of compact stars has been studied by many authors in recent years [16–20]. In Ref. [9] vector interactions are included in the quark EoS, and stable hybrid star configurations with color superconducting quark cores are possible. The authors of Ref. [10] found that assuming a sharp phase transition between hadronic and quark matter, the condition $M_{\rm max} > 2M_\odot$ puts strong constraints on the EoSs of the two-flavor superconducting (2SC) phase and/or the three flavor color-flavor locked (CFL) phase. It was found that strong additional hyperon repulsion is necessary, and the density discontinuity at the hadron-quark interface ought to be small, while the speed of sound in quark matter has to be large. In addition, several recent studies have shown that a third family of massive hybrid stars (so-called twin stars) could exist, by using the NJL quark model with multiquark interactions [21], a chiral SU(3) EoS derived from the quark-meson model [22], a multi-polytrope EoS [23], or based on the relativistic string-flip model (which is a mean-field modification to the free Fermi gas model) [24]. Other authors have obtained twin-stars for three-flavor quark matter, with masses lower than $2M_\odot$ [25, 26]. The inclusion of a very strong magnetic field ($\sim 10^{19}$ G) in the quark matter EoS can also

lead to the appearance of a third family of stable hybrid stars [27]. In Ref. [28], a systematic study of the location of the phase transition between the hadronic matter and quark matter occurs in the "constant-sound-speed" (CSS) [29, 30] parameter space was performed by scanning the transition pressure $p_{\rm trans}$ and the discontinuity in the energy density $\Delta\varepsilon/\varepsilon_{\rm trans}$ between two phases.

In order to study the effects of color superconductivity on the stability of compact stars and search for possible twin-star configurations, we consider the 2SC+s phase, where green and red up and down quarks form pairs, embedded in a gas of free strange quarks, and strange quarks can form pairs amongst themselves [31, 32]. We assume a sharp first-order phase transition between hadronic matter and color superconducting quark matter in order to compare the analysis of the stability of hybrid stars with that in the framework of the CSS parametrization [29, 30]. For the hadronic phase we apply several EoSs based on the non-linear relativistic mean field model proposed in [33]; quark matter in 2SC+s quark phase is described within the local Nambu-Jona Lasinio model (see Sects. II A and II B and for details). As was pointed out in [26, 28, 30, 33, 34], a lower transition pressure together with a not too large discontinuity in the energy density at the phase transition favors the formation of stable hybrid star branches. In this work we will show that, in the context of NJL 2SC+s color superconducting quark phase, a combination of diquark condensates, large values of the vector and diquark interaction, and large effective strange quark masses lowers the hadron-quark transition pressure leading to stable hybrid branches which could be connected, disconnected, or both.

The article is organized as follows. In Sec. II we discuss some basic aspects of phase transitions, and give a brief description of both the hadronic and quark matter EoS as well as the CSS parametrization. In Sec. III we show the

numerical results for different hadronic EoSs and parameter combinations of the 2SC+s quark matter in the CSS framework. In addition, we discuss the results obtained taking into account constraints on the behavior of dense matter from astrophysical observations. Conclusions are provided in Sec. IV.

II. PHASE TRANSITIONS

It has been suggested that at low temperatures and high densities there might be a first-order phase transition between hadronic and quark matter inside neutron stars [35–41]. Although the density at which such a phase transition occurs is unknown it is expected to be several times the nuclear saturation density.

Depending on the value of the surface tension at the hadron-quark interface, this kind of phase transition can lead to two possible stellar configurations [42–48]. If the surface tension is higher than a critical value, which is estimated to be around 5 to 40 MeV/fm² [42, 45], then there is a sharp interface (Maxwell construction) between neutral hadronic matter and neutral quark matter; if the surface tension is below such critical value, there exists a mixed phase (Gibbs construction) with global charge conservation, and the pressure varies monotonically during the phase transition. In this work we assume that the surface tension is high enough to ensure the occurrence of a sharp interface. For a discussion of generic equations of state that continuously interpolate between the phases to model mixing or percolation, see [49–51].

A. Hadronic matter EoS

We have used several EoSs to describe hadronic matter in the interior of hybrid stars. The crust region is constructed by combining the Baym-Bethe-Pethick and Baym-Pethick Sutherland EoSs [52, 53]. The EoS of the outer core region is modeled using the well-known nonlinear relativistic mean field (RMF) theory in which baryons interact via the exchange of scalar (σ), vector (ω), and isovector (ρ) mesons [54–56], and for which numerous nuclear parametrizations exist. First we calculate the hadronic EoS using the NL3 parametrization with the standard set of RMF parameters initially fit to properties of finite nuclei [57]. Hyperons were considered with the following meson-hyperon coupling constants: $x_{\sigma B} = 0.7$ and $x_{\omega B} = x_{\rho B} = 1.0$, where $x_{iB} = g_{iB}/g_i$ [58].

A second hadronic EoS is constructed using the RMF theory with the GM1 parametrization [59], but modified to include a density-dependent isovector meson-baryon coupling constant [60],

$$g_{\rho B}(n) = g_{\rho B}(n_0) \exp[-a_\rho (n/n_0 - 1)]. \qquad (1)$$

This modification provides the extra parameter a_ρ used to fix the slope of the asymmetry energy (L) at nuclear

density (L_0), but leaves the remaining saturation parameters of the original GM1 parametrization intact [61]. In this work we fix $L_0 = 55$ MeV, a value consistent with a number of constraints from the literature (e.g. [62–65]), and refer to this parametrization as GM1(L) [66]. Reducing the slope of the asymmetry energy softens the low density region of the equation of state, decreasing the neutron star radius such that the mass-radius relation of the modified GM1(L) parametrization is consistent with bounds suggested by neutron matter calculations [63]. Hyperons are included with vector meson-hyperon coupling constants given by the SU(3) flavor symmetry, isovector couplings given by the SU(6) relations, and scalar couplings fit to the following hypernuclear potentials: $U_\Lambda^{(N)} = -28$ MeV, $U_\Sigma^{(N)} = 30$ MeV, and $U_\Xi^{(N)} = -18$ MeV [67, 68]. Delta isobars ($\Delta(1232)$) are also included with $x_{\sigma\Delta} = x_{\omega\Delta} = 1.1$ and $x_{\rho\Delta} = 1.0$.

Next we use an RMF model with density-dependent scalar, vector, and isovector meson-baryon coupling constants [60]. The functional density dependence of the couplings requires an additional nine parameters that are fit to properties of finite nuclei and provided by the DD2 parametrization [69, 70]. Nonlinear cubic and quartic scalar self-interaction contributions to the Lagrangian, necessary to reproduce reasonable values of the nuclear incompressibility and effective nucleon mass at saturation with the NL3 and GM1(L) parametrizations, are no longer required. Only nucleons are considered with the DD2 parametrization.

Finally, we test four additional parametrizations for the hadronic EoS to obtain a hadron-quark phase transition: SFHo and SFHx, parametrized to control the isospin asymmetry energy as a function of density and satisfy the initial mass constraint set by PSR J1614–2230 [5, 71], and BHBΛϕ (BHBΛ) including the lambda hyperon with (without) the repulsive hyperon-hyperon interaction mediated by the ϕ meson [72].

B. 2SC+s quark matter EoS

It is known that the constraint from charge neutrality disfavors the 2SC phase, but a large enough strange quark mass helps to stabilize such a superconducting phase [17, 32]. In this work, the 2SC+s superconducting quark phase is described within the two-flavor 2SC Nambu-Jona Lasinio model including vector interactions in a background of strange quarks, with a large constituent strange quark mass.

Although in our model the dynamical strange quark mass is not treated as in the standard NJL model with three flavors, the effective mass of the strange quark, $M_s(\mu)$, is taken as a chemical potential (μ-dependent) parameter. The *ad-hoc* dependence of the effective strange quark mass is described by

Table I. Properties of compact stars arising from the hybrid EoS: NL3 plus 2SC+s (for $M_s^0 = 500$ MeV, $\Delta_s = 10$ MeV, and $\eta_{qq} = 1.1$). We show the parameter values for the phase transition, $p_{\text{trans}}/\varepsilon_{\text{trans}}$ and $\Delta\varepsilon/\varepsilon_{\text{trans}}$, varying the vector coupling constant η_v. The value $\langle c_{\text{QM}}^2 \rangle$ is obtained by calculating the slope of the quark EoS through a linear fitting. We also give the mass and radius of the heaviest hadronic star (M_{trans} and R_{trans}), the mass and radius range (ΔM and ΔR) of the hybrid branch, calculated from the 2SC+s EoS and the CSS parametrization separately. For CSS we pick up the minimum or maximum of the speed of sound for quark matter and assume a constant c_{QM}^2 to be of that value. We found that with $\eta_{qq} = 1.1$ and $\eta_v = 0.85$ both stable connected and disconnected (twin stars) hybrid branches are generated. The masses are expressed in $M_\odot$ and the radii in kilometers.

η_{qq}	η_v	p_t/ε_t	$\Delta\varepsilon/\varepsilon_t$	$\langle c_{\text{QM}}^2 \rangle$		M_{trans}	R_{trans}	$\Delta M_{\text{2SC+s}}$		ΔM_{CSS}	$\Delta R_{\text{2SC+s}}$		ΔR_{CSS}
1.1	0.80	0.147	0.510	0.360		1.73	14.82	0.12		(0.035, 0.48)	−3.27		(−1.51, −3.10)
1.1	0.82	0.164	0.528	0.360		1.84	14.82	0.06		(0.017, 0.215)	−2.42		(−1.37, −2.82)
1.1	0.85	0.186	0.521	C 0.325	D 0.375	1.98	14.79	C 0.008	D 0.006	(0.005, 0.04)	C −0.16	D −1.38	(−0.13, −1.85)

$$\text{M}_s(\mu) = 200 \left[\frac{1}{2} + \frac{1}{2}\tanh\left(\frac{\mu - \widetilde{\mu}}{\beta}\right) \right]$$
$$+ \text{M}_s^0 \left[\frac{1}{2} - \frac{1}{2}\tanh\left(\frac{\mu - \widetilde{\mu}}{\beta}\right) \right], \qquad (2)$$

where $\widetilde{\mu} = 530$ MeV and $\beta = 5 \times 10^2$ MeV. In this functional form of the strange effective mass, a rapid change from an almost constant value of M_s^0 to a value of ~ 200 MeV occurs for a quark chemical potential $\sim \widetilde{\mu}$. This behavior is consistent with the results of [73]. Adopting the change of the strange quark mass as described by Eq. (2) allows us to study the influence of strangeness in the system in a relatively simple manner that retains qualitative and quantitative features of more complex approaches, where a SU(3) NJL Lagrangian with a t'Hooft interaction term and vector interaction is used to determine the strange quark mass self-consistently [9, 17]. Pairing among strange quarks themselves is also allowed, while with the choice of $\text{M}_s(0) \equiv \text{M}_s^0 = 500$ to 600 MeV, we force the strange quarks to remain heavy even at higher densities which inhibits the possibility of them pairing with non-strange quarks. From here onwards we will refer M_s^0 as the initial value of the effective strange quark mass for chemical potentials lower than ~ 550 MeV.

At zero temperature, quark matter in the 2SC+s phase with vector interactions is described in terms of the grand canonical potential

$$\Omega_{\text{2SC+s}} = \Omega_0 + \Omega_{\text{lep}} + \Omega_s + \frac{\sigma^2}{2G_S} + \frac{\Delta^2}{2H} - \frac{\xi^2}{2G_V}$$
$$- \frac{2}{\pi^2}\int_0^\Lambda p^2 \mathrm{d}p \left(E(p) + E_+(p) + E_-(p)\right)$$
$$- \frac{1}{\pi^2}\int_0^{p_F^{(ub)}} p^2 \mathrm{d}p \left[\mu_{(ub)} - E(p)\right] \qquad (3)$$
$$- \frac{1}{\pi^2}\int_0^{p_F^{(db)}} p^2 \mathrm{d}p \left[\mu_{(db)} - E(p)\right],$$

where Ω_0 is a constant fixed by the condition that $\Omega_{\text{2SC+s}}$ vanishes at $\mu = T = 0$, Ω_{lep} is the lepton contribution (we have included both electrons and muons), Ω_s is the contribution from the s quark, $p_F^{(ub)}$ and $p_F^{(db)}$ are the common Fermi momenta for the blue u and d quarks respectively and $E(p) = \sqrt{p^2 + m(\sigma)^2}$, $\bar{\mu} = (\mu - \xi) - \frac{\mu_e}{6} + \frac{\mu_8}{3}$, $E_\pm(p) = \sqrt{[E(p) \pm \bar{\mu}]^2 + \Delta^2}$. The effective mass in the chiral condensate σ is given by $m(\sigma) = m_{i=u=d} - 2G_S\sigma$. G_S, H and G_V are the strong, diquark and vectorial coupling constants respectively. Finally, ξ is the mean field related with the vector interaction included in the model.

Blue strange quarks do not pair, so they are treated as a Fermi quark gas. Red and green strange quarks form pairs, contributing to the grand canonical potential Eq. (3) through a term given by

$$\Omega_s^{\text{red,green}} = \frac{1}{\pi^2}\int_0^{k_F^s} \mathrm{d}p\,p^2 \left[\sqrt{p^2 + \text{M}_s^2 + \Delta_s^2} - \mu_s\right], (4)$$

where M_s is the μ-dependent effective strange quark mass taken as a free parameter and k_F^s is the common Fermi momenta. We choose the parameter values as $m_u = m_d = 5.5$ MeV, $G_S = 10.1 \times 10^{-6}$ MeV and $\Lambda = 650$ MeV in the NJL model [74, 75].

The mean field values σ, ξ, and Δ are obtained by minimizing the grand canonical potential Eq. (3), *i.e.*

$$\frac{\mathrm{d}\Omega_{\text{2SC+s}}}{\mathrm{d}\Delta} = 0, \quad \frac{\mathrm{d}\Omega_{\text{2SC+s}}}{\mathrm{d}\sigma} = 0, \quad \frac{\mathrm{d}\Omega_{\text{2SC+s}}}{\mathrm{d}\xi} = 0. \quad (5)$$

Imposing electric and color charge neutrality by minimizing the potential with respect to the electron and color chemical potentials, μ_e and μ_8, we have

$$\frac{\mathrm{d}\Omega_{\text{2SC+s}}}{\mathrm{d}\mu_e} = 0, \quad \frac{\mathrm{d}\Omega_{\text{2SC+s}}}{\mathrm{d}\mu_8} = 0. \qquad (6)$$

Therefore, Eqs. (5) and (6) form a system of five equations that will be solved together to model the quark matter phase in the inner core of the hybrid star.
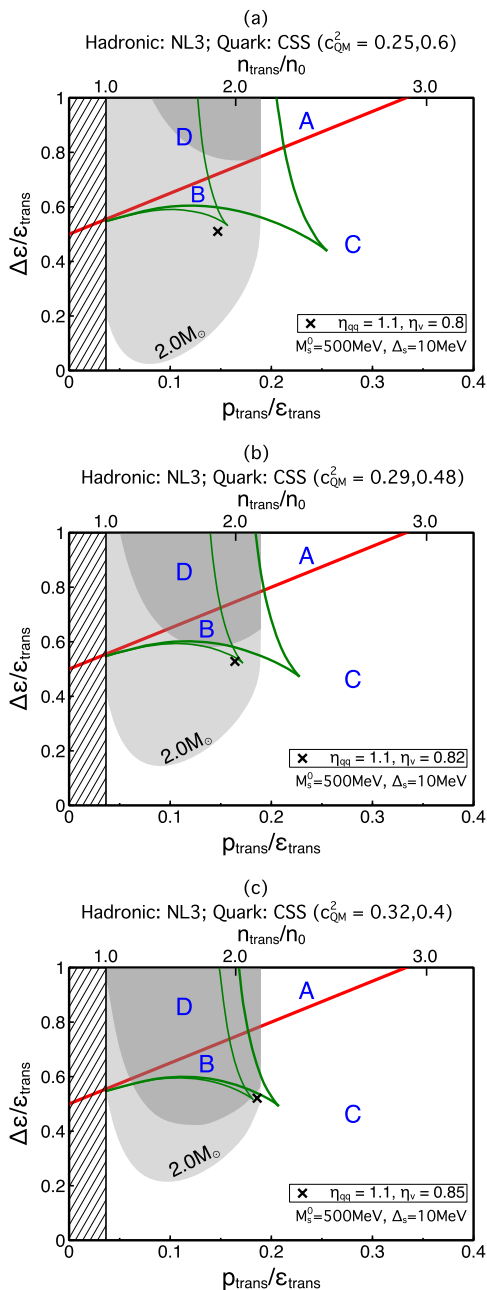
Figure 2. (Color online) Diagram showing (black symbols) where phase transition between NL3 EoS and 2SC+s quark EoS with various parameter values (see Table I and Fig. 4, panel (a)) fall in the CSS parameter space. Each panel is for a different range of c_{QM}^2. EoSs below the straight solid (red) line (regions B and C) yield a connected hybrid branch; EoSs above the (green) window (regions B and D) yield a disconnect hybrid branch. EoSs within the shaded gray area are excluded because their heaviest star is below $2M_\odot$.

C. CSS parametrization

The "constant-sound-speed" framework enables a generic analysis of the stability of hybrid stars [30]. For a given nuclear matter EoS, $\varepsilon_{NM}(p)$, the full CSS EoS is then

$$
\varepsilon(p) = \begin{cases} \varepsilon_{NM}(p) & p < p_{trans} \\ \varepsilon_{NM}(p_{trans}) + \Delta\varepsilon + c_{QM}^{-2}(p - p_{trans}) & p > p_{trans}. \end{cases}
\tag{7}
$$

The CSS form can be viewed as the lowest-order terms of a Taylor expansion of the high-density EoS about the transition pressure. We express the three parameters in dimensionless form, as $p_{trans}/\varepsilon_{trans}$, $\Delta\varepsilon/\varepsilon_{trans}$ (equal to $\lambda - 1$ in the notation used in [76]) and c_{QM}^2, where $\varepsilon_{trans} \equiv \varepsilon_{NM}(p_{trans})$.

As we will show later in Sec. III, EoS models considered in this work can give rise to values of $p_{trans}/\varepsilon_{trans} \sim 0.14 - 0.19$ and $\Delta\varepsilon/\varepsilon_{trans} \sim 0.04 - 0.7$ in the CSS framework. With these ranges of parameters, which characterize the location of the phase transition, stable hybrid stars are obtained. This is the major difference from previous results in [33] where local and non-local NJL models without diquarks were used to describe the quark matter EoS. In that work, both the phase transition pressure p_{trans} and the energy discontinuity $\Delta\varepsilon$ were too high to obtain stable hybrid stars with quark matter cores, in agreement with the predictions from the CSS parametrization. The inclusion of diquarks in the NJL model instead helps both lower the transition pressure and shrink the gap in the energy density, and thus favors a stable hybrid star configuration. At this point, it is worth to point out that stable hybrid stars with quark matter in their cores and maximum masses above $2M_\odot$ have already been obtained for the local NJL model, if deconfinement and the chiral phase transition occur at the same chemical potential [77]. The authors of this paper note that this condition together with a low vacuum constituent quark mass are essential to obtain hybrid stars with pure quark matter in their cores when Gibbs conditions are considered.

In Fig. 1 we show the square of the speed of sound, c_{QM}^2, in the quark matter phase as a function of the pressure for two different effective strange quark masses $M_s^0 = 500, 600$ MeV. For a given M_s^0, the speed of sound increases slightly with the vector coupling constant η_v, and more significantly with the diquark coupling constant η_{qq}. The first peak of c_{QM}^2 on these curves, more evident for $M_s^0 = 600$ MeV, occurs at the blue strange quark onset, representing a change in the properties of the matter inside the compact star. The second peak corresponds to the appearance of the strange diquarks. In Tables. I and II we compute an estimate mean value of the square speed of sound $\langle c_{QM}^2 \rangle$ through a linear fitting to the quark EoS $\varepsilon(p)$ (only for values giving stable stars); the inverse of the linear fitting slope is taken as $\langle c_{QM}^2 \rangle$.

(a)
Hadronic: NL3; Quark: CSS ($c_{QM}^2 = 0.25, 0.64$)

(b)
Hadronic: NL3; Quark: CSS ($c_{QM}^2 = 0.29, 0.45$)

(c)
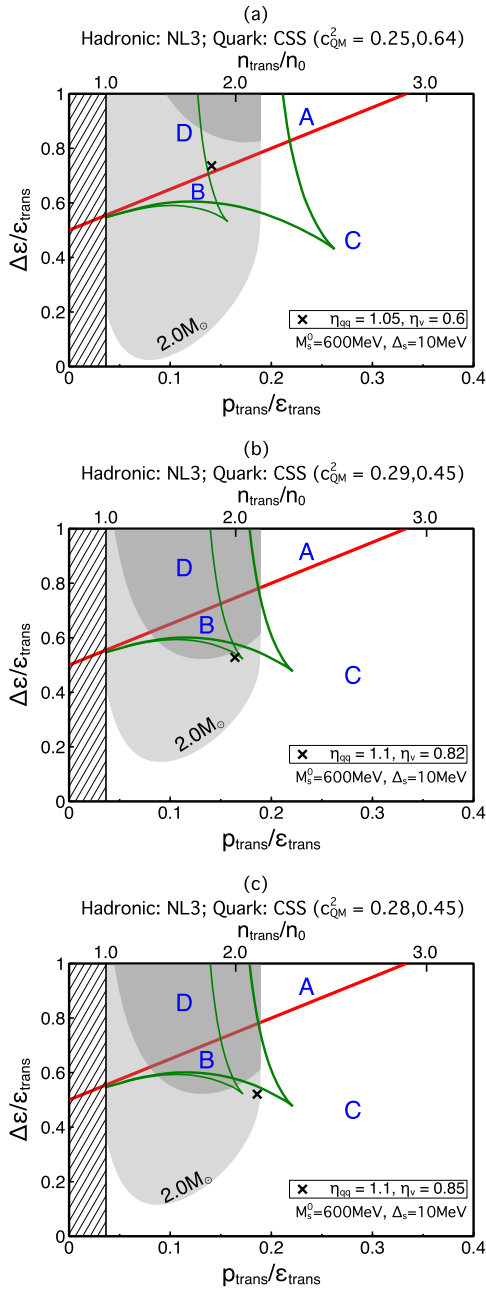## Hadronic: NL3; Quark: CSS ($c_{QM}^2 = 0.28, 0.45$)

Figure 3. (Color online) Diagram showing (black symbols) where phase transition between NL3 EoS and 2SC+s quark EoS with various parameter values (see Table II and Fig. 4, panel (b)) fall in the CSS parameter space. Each panel is for a different range of c_{QM}^2. EoSs below the straight solid (red) line (regions B and C) yield a connected hybrid branch; EoSs above the (green) window (regions B and D) yield a disconnect hybrid branch. EoSs within the shaded gray area are excluded because their heaviest star is below $2M_\odot$.

III. HYBRID STARS WITH COLOR SUPERCONDUCTING CORES

Considering a sharp first-order phase transition we are able to construct hybrid EoSs and solve the TOV equations to find stable configurations of compact stars. We then analyze the effect of the vector interaction, the superconducting coupling constant, the role of the strange quark mass and the possibility of a superconducting quark matter core in hybrid stars.
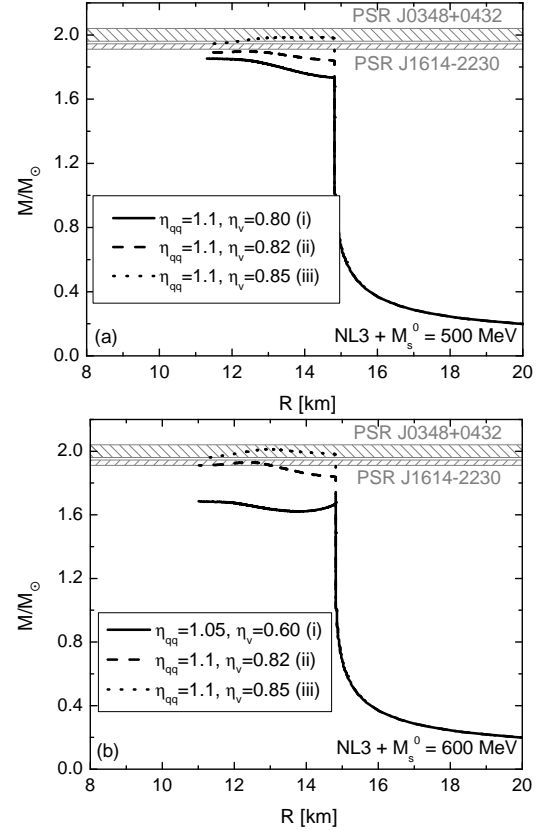

Figure 4. Mass-radius relationship for hybrid stars using an effective strange quark mass $M_s^0 = 500$ MeV (a), $M_s^0 = 600$ MeV (b), and the superconducting gap for the strange quark $\Delta_s = 10$ MeV. We use NL3 for the hadronic EoS, and quantities that characterize the phase transition to the 2SC+s phase are shown in Tables I and II. Variation of the speed of sound in the quark phase is shown in Fig. 1. Labels (i), (ii) and (iii) are in accordance with the corresponding (a), (b) and (c) CSS diagrams in Figs. 2 and 3.

A. NL3 hadronic EoS

In Tables I and II we show the relevant quantities for the 2SC+s model considering the phase transition with the NL3 hadronic EoS for a given effective strange quark mass ($M_s^0 = 500$ and 600 MeV respectively). Comparison with the results obtained from the CSS parametrization

Table II. Properties of the compact stars arising from the hybrid EoS: NL3 plus 2SC+s (for $M_s^0 = 600$ MeV and $\Delta_s = 10$ MeV). We show the parameter values for the phase transition, $p_{\text{trans}}/\varepsilon_{\text{trans}}$ and $\Delta\varepsilon/\varepsilon_{\text{trans}}$, varying the vector coupling constant η_v and the diquark coupling constant η_{qq}. The value $\langle c_{\text{QM}}^2 \rangle$ is obtained by calculating the slope of the quark EoS through a linear fitting. We also give the mass and radius of the heaviest hadronic star (M_{trans} and R_{trans}), the mass and radius range (ΔM and ΔR) of the hybrid branch, calculated from the 2SC+s EoS and the CSS parametrization separately. For CSS we pick up the minimum or maximum of the speed of sound for quark matter and assume a constant c_{QM}^2 to be of that value. The masses are expressed in $M_\odot$ and the radii in kilometers.

η_{qq}	η_v	p_t/ε_t	$\Delta\varepsilon/\varepsilon_t$	$\langle c_{\text{QM}}^2 \rangle$	M_{trans}	R_{trans}	$\Delta M_{\text{2SC+s}}$	ΔM_{CSS}	$\Delta R_{\text{2SC+s}}$	ΔR_{CSS}
1.05	0.60	0.141	0.736	0.360	1.67	14.82	0.02	$\lesssim 0.36$	-4.42	$\gtrsim -3.75$
1.1	0.82	0.164	0.528	0.400	1.84	14.82	0.11	$(0.017, 0.182)$	-2.70	$(-1.37, -2.71)$
1.1	0.85	0.186	0.521	0.400	1.98	14.79	0.04	$(0.005, 0.078)$	-1.79	$(-0.09, -2.33)$

is also given, where maximum and minimum values of ΔM_{CSS} and ΔR_{CSS} correspond to the extremes of c_{QM}^2 in the stable hybrid branches.

We have noticed that changes in the choice of the effective strange quark mass M_s^0 do not alter the transition pressure from hadronic matter to quark matter; however increasing M_s^0 stiffens the quark matter EoS. There is no variation of the transition point when the gap parameter Δ_s changes, but greater values of Δ_s make the EoS (slightly) stiffer, although the difference is practically insensitive. Regarding the diquark coupling constant η_{qq}, we have found that when $\eta_{qq} < 1$ all stable stars are purely hadronic (same result as obtained in [33]); on the contrary, when $\eta_{qq} > 1$ hybrid star branches (connected, disconnected or both) are present. Fixing η_{qq} and increasing the vector coupling constant η_v leads to a stiffer EoS (see more evidently in Fig. 1), and at the same time shifts the transition point to higher pressures and disfavor the formation of a quark matter core.

In Fig. 4 (a), we show mass-radius relation for different choices of the model parameters. Fixing $M_s^0 = 500$ MeV, $\Delta_s = 10$ MeV and $\eta_{qq} = 1.1$, we vary the vector coupling constant as $\eta_v = 0.80, 0.82, 0.85$. As shown in Table I the transition pressure p_{trans} between hadronic matter and quark matter increases with η_v, which results in a higher mass for the heaviest purely-hadronic star $M = M_{\text{trans}}$.

For all these cases, there always exists a connected branch of hybrid stars right above the transition pressure p_{trans}. In particular for $\eta_v = 0.85$ (dotted curve), a disconnected hybrid branch is also present, and a maximum mass $\sim 2M_\odot$ is reached. For $\eta_v = 0.80$ and $\eta_v = 0.82$ only connected hybrid branches exist.
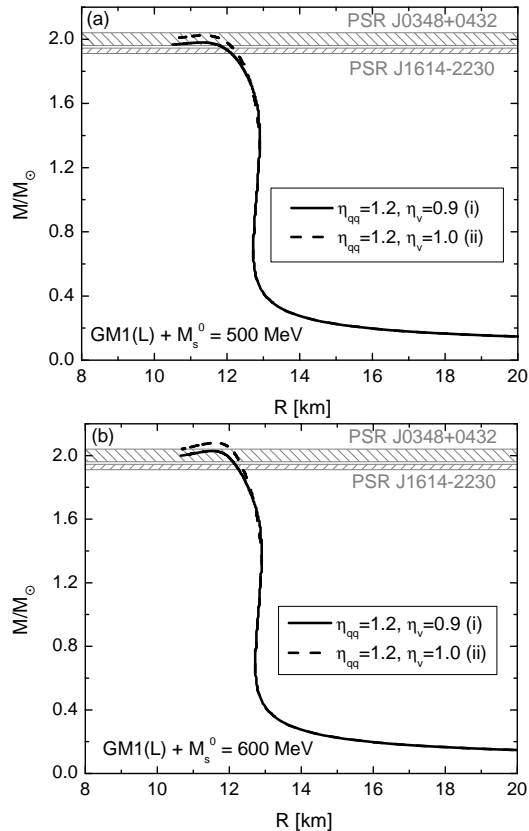

Figure 5. Mass-radius relationship for hybrid stars using an effective strange quark mass $M_s^0 = 500$ MeV (a), $M_s^0 = 600$ MeV (b), and the superconducting gap for the strange quark $\Delta_s = 50$ MeV. We use GM1(L) for the hadronic EoS, and quantities that characterize the phase transition to the 2SC+s phase are shown in Tables III and IV. Variation of the speed of sound in the quark phase is shown in Fig. 1. Labels (i) and (ii) are in accordance with the corresponding (a), (c) and (b), (d) of the CSS diagrams in Fig. 6.

Fig. 4 (b) displays the mass-radius relation for hybrid star configurations fixing $M_s^0 = 600$ MeV and $\Delta_s = 10$ MeV. The cases where $\eta_{qq} = 1.1$, $\eta_v = 0.82$ and $\eta_v = 0.85$ (dashed and dotted curves) are similar to those in panel (a) with connected hybrid branches and

slightly higher maximum mass because the quark EoS stiffens when M_s^0 increases (see Fig. 1). Both curves are consistent with the observational data of the two $\sim 2M_\odot$ pulsars. For $\eta_{qq} = 1.05$ and $\eta_v = 0.6$ (solid line), as also can be seen in Table II, lower values of both the diquark and vector coupling constants result in a lower transition pressure and a lower mass for the heaviest purely-hadronic star. A disconnected branch of stars with color superconducting cores is present, but its maximum mass is below $2M_\odot$.

One remarkable feature of Fig. 4 is that hybrid stars with color superconducting quark cores have systematically smaller radii than purely hadronic stars, a result of the first-order phase transition in dense matter that has been widely discussed. For instance, Ref. [78] shows that if hybrid EoSs are constructed with extremely stiff hadronic matter at transition densities around 1.5 times nuclear saturation density, disconnected hybrid branches covered a range of $2 - 3$ kilometers smaller than the purely-hadronic branch.

In Fig. 2 we show with crosses the phase transition points corresponding to the 2SC+s EoS for $M_s = 500$ MeV model combined with NL3 hadronic EoS. For the lowest and highest values of c_{QM}^2 realized in stable stellar configurations, we calculate the $M_{max} = 2M_\odot$ contours and the twin-star windows demarcating the disconnected branches. An interesting transition point as in panel (c) indicates hybrid star configurations very close to the edge of region B, where both disconnected and connected hybrid branches should exist, which is confirmed in the actual mass-radius relation for 2SC+s models (see dotted curve in Fig. 4 (a)). It is worth mentioning that the reason why at this phase transition point both branches (represented by region "B") do not appear for the CSS parametrization in Fig. 2 (c) is that c_{QM}^2 is not strictly constant in the 2SC+s phase. This could be seen in a 3-D diagram, with c_{QM}^2 gradually varying along a third axis, while the phase transition point $(p_{trans}/\varepsilon_{trans}, \Delta\varepsilon/\varepsilon_{trans}, c_{QM}^2(p = p_{trans}))$ lies in the twin-star window (a 2-D plane). In Fig. 3 we show the same but for $M_s = 600$ MeV. Panel (a) represents a typical case of disconnected family of hybrid stars (in region D above the solid red line) but with a maximum mass below the $2M_\odot$ threshold (within the gray excluded area), which refers to the red solid curve in Fig. 4 (b).

To obtain massive ($\gtrsim 2M_\odot$) hybrid stars on the disconnected branch, the range of parameters combination is quite narrow; it is very difficult but not impossible. In the EoS models considered, high values of the diquark coupling constant and the vector interaction coupling ensure relatively low transition pressures, which are favored to generate stable hybrid stars as predicted from the CSS parametrization. Similarly, in a previous work, massive twin hybrid stars have been obtained by including higher-order quark interactions in the Dirac scalar and vector coupling channels [78]; these interactions also effectively rebound to lower transition pressures and large values of c_{QM}^2, although they additionally have high M_{trans} due to
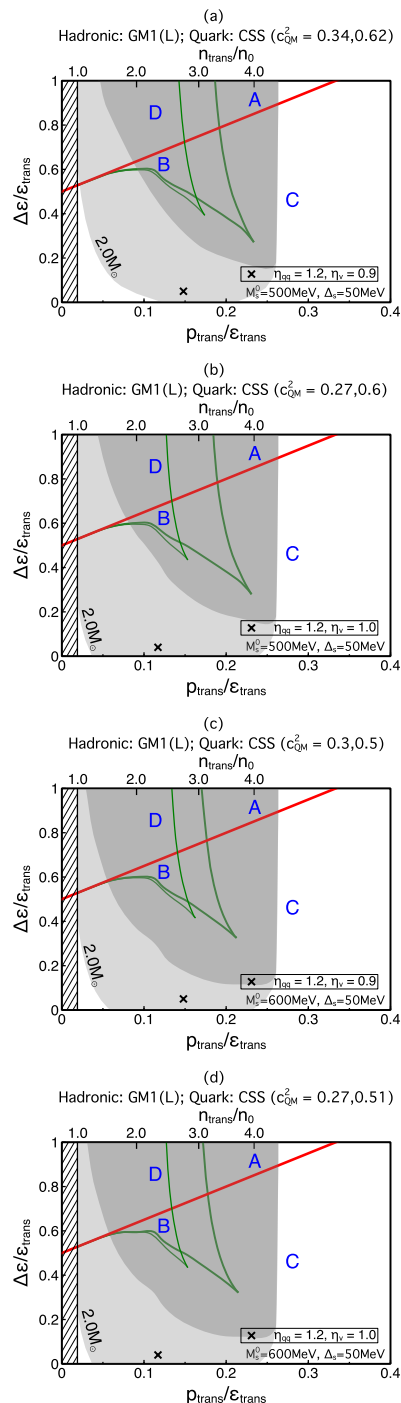

Figure 6. (Color online) Diagram showing (black symbols) where phase transition between GM1(L) EoS and 2SC+s quark EoS with various parameter values (panels (a) & (b): Table III; panels (c) & (d): Table IV) fall in the CSS parameter space. Each panel is for a different range of c_{QM}^2. EoSs below the straight solid (red) line (regions B and C) yield a connected hybrid branch; EoSs above the (green) window (regions B and D) yield a disconnect hybrid branch. EoSs within the shaded gray area are excluded because their heaviest star is below $2M_\odot$.

the extremely stiff DD2-EV hadronic EoS.

B.   GM1(L) hadronic EoS

The GM1 parametrization has been widely used for the description of nuclear matter in neutron stars (see for example [79, 80] and references therein), however its continued utility may be questionable in light of recent constraints placed on the slope of the isospin asymmetry energy and neutron star radii.

Therefore, in this work we use the modified version of the GM1 parametrization (GM1(L)) discussed in Subsection III B which is more consistent with these constraints and with results from microscopic neutron matter calculations. In Table III and IV we show the results obtained using the GM1(L) parametrization for the hadronic phase. It can be seen that hybrid stars with color superconducting quark matter cores are possible and that quark matter appears not only in the cores of high mass hybrid stars but also in intermediate mass compact objects. This is also shown in Fig. 6 where the gray shaded region is excluded by the measurement of the $2M_\odot$ stars. We obtain connected hybrid branches with color superconducting cores with masses below $2M_\odot$, but still within the error bars, of PSR J1614–2230 and PSR J0348+0432. In contrast, a previous study of hybrid stars obtained with the GM1 EoS using the CSS parametrization [33] led to very short connected or absent hybrid branches for $2M_\odot$ neutron stars.

C.   DD2 and other hadronic EoS

The results obtained using the DD2 parametrization for the hadronic EoS are shown in Table V, where stable hybrid stars with color superconducting quark matter cores only appear on the connected branch. We show the mass-radius relation in Fig. 7 (a), and mass as a function of the central energy density in Fig. 7 (b). Compared to the results from the NL3 hadronic EoS (see Fig. 4), these hybrid stars have higher masses, smaller radii and shorter connected branches compared with GM1(L). Fig. 8 shows the results on the CSS plane ($p_{\rm trans}/\varepsilon_{\rm trans}$, $\Delta\varepsilon/\varepsilon_{\rm trans}$) where only for panel (a) with $\eta_{\rm qq} = 1.1$ and $\eta_{\rm v} = 0.65$ are stars obtained that have maximum masses $< 2M_\odot$ (transition point inside the gray shaded area).

Similar calculations were performed using the SFHo and SFHx parametrizations and the BHBΛφ (BHBΛ) parametrizations including Λ hyperons with (without) repulsive interactions [72]. For SFHo and SFHx EoS, disconnected families of hybrid stars are possible (for example, if vector interactions are strong ($\eta_{\rm v} > 0.5$) with the strange quark mass $M_{\rm s}^0 = 500$, the phase transition parameters are $p_{\rm trans}/\varepsilon_{\rm trans} \sim 0.2$ and $\Delta\varepsilon/\varepsilon_{\rm trans} \sim 0.55$), but in neither case does the maximum mass reach the limit imposed by the measurements of J1614–2230 [5, 6] and J0348+0432 [7].
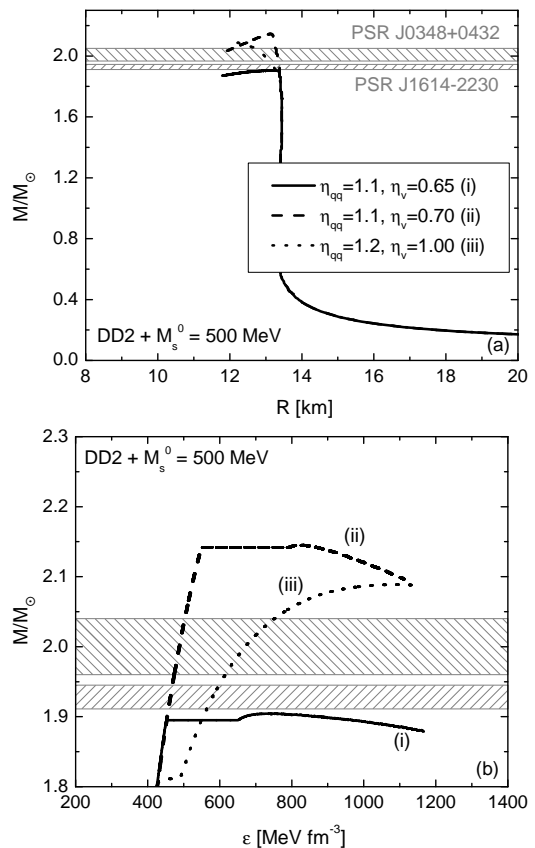

Figure 7.   Hybrid star configurations based on the DD2 hadronic EoS and quark matter EoS with the effective strange quark mass $M_{\rm s}^0 = 500$ MeV, and the superconducting gap for the strange quark, $\Delta_{\rm s} = 50$ MeV. Panel (a): mass-radius curves; panel (b): mass as a function of the central energy density. All curves show connected families of hybrid stars. Labels (i), (ii) and (iii) are in accordance with the corresponding (a), (b) and (c) CSS diagrams in Fig.8. Quantities that characterize the phase transition to the 2SC+s phase are shown in Table V.

In addition, for $M_{\rm s}^0 = 600$ MeV, even by combining and increasing $\eta_{\rm v}$ and/or $\eta_{\rm qq}$, the phase transition itself does not occur. For BHBΛφ and BHBΛ the appearance of a quark matter superconducting core destabilizes the star immediately. The phase transition is only possible if $\eta_{\rm v} < 0.3$ and if $M_{\rm s}^0 < 500$ MeV. In these cases typical phase transition parameters are $p_{\rm trans}/\varepsilon_{\rm trans} \sim 0.2$ and $\Delta\varepsilon/\varepsilon_{\rm trans} > 0.7$, where the presence of a color superconducting phase in the inner core of the hybrid star destabilizes it.

It should be noted that in a recent analysis of cold hybrid stars, using DD2 and BHBΛφ parametrizations for the hadronic phase and an MIT bag model with the CSS parametrization for the quark matter, $M_{\rm max} \gtrsim 2M_\odot$ for the disconnected hybrid branch are obtained only in a narrow parameter space [28]. This study can be interesting for future supernovae EoS candidates.
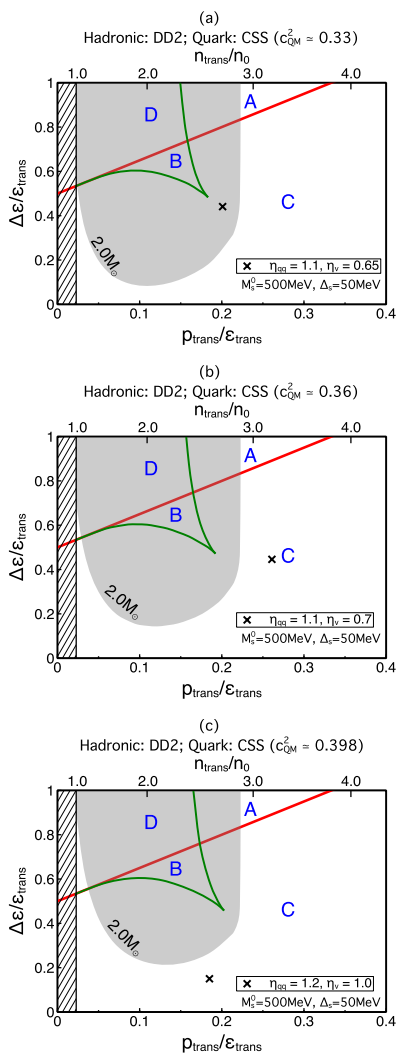
Figure 8. (Color online) Diagram showing (black symbols) where phase transition between DD2 EoS and 2SC+s quark EoS with various parameter values (see Table V) fall in the CSS parameter space. Each panel is for a different value of $c^2_{QM} \approx \langle c^2_{QM} \rangle$. EoSs below the straight solid (red) line (regions B and C) yield a connected hybrid branch; EoSs above the (green) window (regions B and D) yield a disconnect hybrid branch. EoSs within the shaded gray area are excluded because their heaviest star is below $2M_\odot$. Only panels (b) and (c) predict phase transitions that ensure $M_{max} > 2M_\odot$, consistent with (ii) and (iii) curves in Fig. 7.

IV. CONCLUSIONS

In this work we have analyzed the existence of connected, disconnected or both simultaneously stable hybrid star branches considering the 2SC+s color superconducting phase for the description of quark matter. Our results confirm that a 2SC+s color superconducting quark phase in the framework of local NJL models where diquark condensates lower the phase transition pressure can give rise to stable hybrid stars with quark cores,

as expected in a previous work [33]. However, the parameter space for quark EoSs to be compatible with the $M_{max} \gtrsim 2M_\odot$ constraint is fairly restricted, and not for all the hadronic EoSs we considered either.

Although we find that disconnected branches (third family) of hybrid stars could exist for some of the hadronic EoSs used in this paper, masses of these twin stars are below $2M_\odot$; massive stars with $\sim 2M_\odot$ are possible only on the connected branch. Similar results were found in the previous study [26], where the authors applied the Field Correlator Method for three flavors of quarks but did not include the possibility of diquark pair formation. In contrast, with extremely stiff hadronic matter as found with the DD2-EV EoS as introduced in [78], hybrid stars on the disconnected branch heavier than $2M_\odot$ are possible, which remains consistent with predictions on the CSS phase diagram [21]. In fairly good agreement with other recent studies carried out for the generic CSS framework e.g. [28, 34], our results reinforce the applicability of the CSS parametrization in hybrid star studies, when a sharp phase transition is considered between hadronic matter and quark matter.

The hybrid star branches (connected or disconnected) obtained with our model cover a large range of radii (ΔR of a couple of kilometers) but a narrow range of masses (ΔM of a few tenths of the maximum solar mass). This is a major difference with respect to the stellar configurations based on most of the hadronic EoSs, which cover a wide range of masses ranging from $\sim M_\odot/2$ up to $\sim 2M_\odot$ at almost constant radius. Our results strengthen the existing idea that accurate measurements of radii of high-mass compact objects are needed in order to break the degeneracy of most stars on the hybrid branch, probably ruling out most of the high-density hadronic EoSs for neutron stars.

We have taken typical values of the constituent strange quark mass at zero baryon chemical potential of $M^0_s = 500$ and 600 MeV and considered an *ad-hoc* functional dependence of the strange quark mass on the baryon chemical potential, which is consistent with the results of Ref. [73]. This choice allow us to study the influence of strangeness in the system in a relatively simple manner, while retaining qualitative and quantitative features of more complex approaches, where the strange quark mass is determined self-consistently We expect that the essential features established in this paper for our model will have their close correspondence in a treatment where a SU(3) NJL Lagrangian with a t'Hooft interaction term and vector interaction would be used to determine the strange quark mass self-consistently [9, 17]. For our 2SC+s model, all the phase transitions from hadronic matter to quark matter occurs for chemical potentials $\mu < 530$ MeV, where the simulated strange quark mass is almost constant.

We have restricted ourselves to studying the phase transition of hadronic matter to two-flavor color superconducting matter, but the possibility of a phase transition of hadronic matter to quark matter in the 2SC or

CFL phases and the influence of the strange quark mass on these transitions has not be studied. Also, we have not considered any mixing terms between up, down and strange quarks because, for NJL-type models, this could lead to a 2SC-CFL phase transition at rather low baryon chemical potentials. In this case, the CFL phase would be the favored condensation pattern of quark matter at low to intermediate densities [17].

[1] J. Antoniadis, T. M. Tauris, F. Ozel, E. Barr, D. J. Champion, and P. C. C. Freire, *The millisecond pulsar mass distribution: Evidence for bimodality and constraints on the maximum neutron star mass*, ArXiv e-prints (2016) [`arXiv:1605.0166`].

[2] F. Özel and P. Freire, *Masses, Radii, and the Equation of State of Neutron Stars*, Annual Review of Astronomy and Astrophysics **54** (2016) 401–440, [`arXiv:1603.0269`].

[3] J. M. Lattimer and M. Prakash, *Neutron star observations: Prognosis for equation of state constraints*, Physics Reports **442** (2007), no. 1?6 109 – 165. The Hans Bethe Centennial Volume 1906-2006.

[4] J. M. Lattimer, *The Nuclear Equation of State and Neutron Star Masses*, Annual Review of Nuclear and Particle Science **62** (2012) 485–515, [`arXiv:1305.3510`].

[5] P. Demorest, T. Pennucci, S. Ransom, M. Roberts, and J. Hessels, *Shapiro Delay Measurement of A Two Solar Mass Neutron Star*, Nature **467** (2010) 1081–1083, [`arXiv:1010.5788`].

[6] E. Fonseca, T. T. Pennucci, J. A. Ellis, I. H. Stairs, D. J. Nice, S. M. Ransom, P. B. Demorest, Z. Arzoumanian, K. Crowter, T. Dolch, R. D. Ferdman, M. E. Gonzalez, G. Jones, M. L. Jones, M. T. Lam, L. Levin, M. A. McLaughlin, K. Stovall, J. K. Swiggum, and W. Zhu, *The nanograv nine-year data set: Mass and geometric measurements of binary millisecond pulsars*, The Astrophysical Journal **832** (2016), no. 2 167.

[7] J. Antoniadis *et. al.*, *A Massive Pulsar in a Compact Relativistic Binary*, Science **340** (2013) 6131, [`arXiv:1304.6875`].

[8] F. Weber, ed., *Pulsars as astrophysical laboratories for nuclear and particle physics*, 1999.

[9] L. Bonanno and A. Sedrakian, *Composition and stability of hybrid stars with hyperons and quark color-superconductivity*, Astron. Astrophys. **539** (2012) A16, [`arXiv:1108.0559`].

[10] J. L. Zdunik and P. Haensel, *Maximum mass of neutron stars and strange neutron-star cores*, Astron. Astrophys. **551** (2013) A61, [`arXiv:1211.1231`].

[11] T. Noda, M.-a. Hashimoto, N. Yasutake, T. Maruyama, T. Tatsumi, and M. Fujimoto, *Cooling of Compact Stars with Color Superconducting Phase in Quark-hadron Mixed Phase*, Astrophys. J.**765** (2013) 1, [`arXiv:1109.1080`].

[12] M. Orsaria, H. Rodrigues, F. Weber, and G. A. Contrera, *Quark-hybrid matter in the cores of massive neutron stars*, Phys. Rev. **D87** (2013), no. 2 023001, [`arXiv:1212.4213`].

[13] M. Orsaria, H. Rodrigues, F. Weber, and G. A. Contrera, *Quark deconfinement in high-mass neutron stars*, Phys. Rev. **C89** (2014), no. 1 015806, [`arXiv:1308.1657`].

[14] I. A. Shovkovy, *Two Lectures on Color Superconductivity*, Foundations of Physics **35** (2005) 1309–1358, [`nucl-th/0410091`].

[15] M. G. Alford, A. Schmitt, K. Rajagopal, and T. Schäfer, *Color superconductivity in dense quark matter*, Reviews of Modern Physics **80** (2008) 1455–1515, [`arXiv:0709.4635`].

[16] M. Alford, *Color-Superconducting Quark Matter*, Annual Review of Nuclear and Particle Science **51** (2001) 131–160, [`hep-ph/0102047`].

[17] M. Buballa, *NJL-model analysis of dense quark matter [review article]*, Physics Reports **407** (2005) 205–376, [`hep-ph/0402234`].

[18] M. G. Alford, *Quark matter in neutron stars*, Nuclear Physics A **830** (2009) 385–392c, [`arXiv:0907.0200`].

[19] C. Vásquez Flores and G. Lugones, *Radial oscillations of color superconducting self-bound quark stars*, Phys. Rev. D**82** (2010), no. 6 063006, [`arXiv:1008.4882`].

[20] G. Pagliara, *Formation of quark phases in protoneutron stars: The transition from the two-flavor color-superconducting phase to the normal quark phase*, Phys. Rev. D**83** (2011), no. 12 125013, [`arXiv:1012.3046`].

[21] D. Alvarez-Castillo, S. Benic, D. Blaschke, S. Han, and S. Typel, *Neutron star mass limit at 2M? supports the existence of a CEP*, European Physical Journal A **52** (2016) 232, [`arXiv:1608.0242`].

[22] A. Zacchi, M. Hanauske, and J. Schaffner-Bielich, *Stable hybrid stars within a su(3) quark-meson-model*, Phys. Rev. D **93** (2016) 065011.

[23] D. E. Alvarez-Castillo and D. B. Blaschke, *High-mass twin stars with a multipolytrope equation of state*, Phys.

Rev. C **96** (Oct, 2017) 045809.

[24] M. A. R. Kaltenborn, N.-U. F. Bastian, and D. B. Blaschke, *Quark-nuclear hybrid star equation of state with excluded volume effects*, Phys. Rev. D **96** (Sep, 2017) 056024.

[25] B. K. Agrawal, *Equations of state and stability of color-superconducting quark matter cores in hybrid stars*, Phys. Rev. D**81** (2010), no. 2 023009, [`arXiv:1001.1584`].

[26] M. G. Alford, G. F. Burgio, S. Han, G. Taranto, and D. Zappalà, *Constraining and applying a generic high-density equation of state*, Phys. Rev. D **92** (2015) 083002.

[27] H. Sotani and T. Tatsumi, *Quark matter with strong magnetic field and possibility of the third family of compact stars*, Mon. Not. R. Astron. Soc. (2017) [`arXiv:1701.0636`].

[28] O. Heinimann, M. Hempel, and F.-K. Thielemann, *Towards generating a new supernova equation of state: A systematic analysis of cold hybrid stars*, Phys. Rev. **D94** (2016), no. 10 103008, [`arXiv:1608.0886`].

[29] J. L. Zdunik, P. Haensel, and R. Schaeffer, *Phase transitions in stellar cores. II - Equilibrium configurations in general relativity*, Astron. Astrophys. **172** (1987) 95–110.

[30] M. G. Alford, S. Han, and M. Prakash, *Generic conditions for stable hybrid stars*, Phys. Rev. **D88** (2013), no. 8 083013, [`arXiv:1302.4732`].

[31] M. Alford, J. Berges, and K. Rajagopal, *Unlocking color and flavor in superconducting strange quark matter*, Nuclear Physics B **558** (1999), no. 1?2 219 – 242.

[32] M. G. Alford, J. A. Bowers, J. M. Cheyne, and G. A. Cowan, *Single color and single flavor color superconductivity*, Phys. Rev. D**67** (2003), no. 5 054018, [`hep-ph/0210106`].

[33] I. F. Ranea-Sandoval, S. Han, M. G. Orsaria, G. A. Contrera, F. Weber, and M. G. Alford, *Constant-sound-speed parametrization for Nambu-Jona-Lasinio models of quark matter in hybrid stars*, Phys. Rev. C**93** (2016), no. 4 045812, [`arXiv:1512.0918`].

[34] A. Zacchi, M. Hanauske, and J. Schaffner-Bielich, *Stable hybrid stars within a SU(3) Quark-Meson-Model*, Phys. Rev. **D93** (2016), no. 6 065011, [`arXiv:1510.0018`].

[35] K. Schertler, C. Greiner, J. Schaffner-Bielich, and T. M. H., *Quark phases in neutron stars and a "third family" of compact stars as a signature for phase transitions*, Nucl. Phys. **A677** (2000) 463, [`astro-ph/0001467`].

[36] E. S. Fraga, R. D. Pisarski, and J. Schaffner-Bielich, *Small, dense quark stars from perturbative QCD*, Phys. Rev. D**63** (2001), no. 12 121702, [`hep-ph/0101143`].

[37] M. Buballa, F. Neumann, M. Oertel, and I. Shovkovy, *Quark mass effects on the stability of hybrid stars*, Phys. Lett. **B595** (2004) 36–43, [`nucl-th/0312078`].

[38] N. Yasutake, R. Łastowiecki, S. Benić, D. Blaschke, T. Maruyama, and T. Tatsumi, *Finite-size effects at the hadron-quark transition and heavy hybrid stars*, Phys. Rev. C**89** (2014), no. 6 065803, [`arXiv:1403.7492`].

[39] B. Agrawal, *Equations of state and stability of color-superconducting quark matter cores in hybrid stars*, Phys.Rev. **D81** (2010) 023009, [`arXiv:1001.1584`].

[40] A. Kurkela, P. Romatschke, and A. Vuorinen, *Cold Quark Matter*, Phys. Rev. **D81** (2010) 105021, [`arXiv:0912.1856`].

[41] R. Negreiros, V. A. Dexheimer, and S. Schramm, *Quark core impact on hybrid star cooling*, Phys. Rev. **C85** (2012) 035805, [`arXiv:1011.2233`].

[42] M. Alford, K. Rajagopal, S. Reddy, and F. Wilczek, *Minimal color-flavor-locked-nuclear interface*, Phys. Rev. D**64** (2001), no. 7 074017, [`hep-ph/0105009`].

[43] K. Iida and K. Sato, *Effects of hyperons on the dynamical deconfinement transition in cold neutron star matter*, Phys. Rev. **C58** (1998) 2538–2559, [`nucl-th/9808056`].

[44] L. F. Palhares and E. S. Fraga, *Droplets in the cold and dense linear sigma model with quarks*, Phys.Rev. **D82** (2010) 125018, [`arXiv:1006.2357`].

[45] T. Endo, *Region of hadron-quark mixed phase in hybrid stars*, Phys. Rev. **C83** (2011) 068801, [`arXiv:1105.2445`].

[46] M. B. Pinto, V. Koch, and J. Randrup, *The Surface Tension of Quark Matter in a Geometrical Approach*, Phys. Rev. **C86** (2012) 025203, [`arXiv:1207.5186`].

[47] G. Lugones, A. G. Grunfeld, and M. Al Ajmi, *Surface tension and curvature energy of quark matter in the Nambu-Jona-Lasinio model*, Phys. Rev. **C88** (2013), no. 4 045803, [`arXiv:1308.1452`].

[48] W.-y. Ke and Y.-x. Liu, *Interface tension and interface entropy in the 2+1 flavor Nambu-Jona-Lasinio model*, Phys. Rev. **D89** (2014), no. 7 074041, [`arXiv:1312.2295`].

[49] T. Kojo, P. D. Powell, Y. Song, and G. Baym, *Phenomenological QCD equation of state for massive neutron stars*, Phys. Rev. **D91** (2015), no. 4 045003, [`arXiv:1412.1108`].

[50] J. Macher and J. Schaffner-Bielich, *Phase transitions in compact stars*, Eur.J.Phys. **26** (2005) 341–360, [`astro-ph/0411295`].

[51] K. Masuda, T. Hatsuda, and T. Takatsuka, *Hadron-quark Crossover and Massive Hybrid Stars with Strangeness*, Astrophys. J.**764** (2013) 12, [`arXiv:1205.3621`].

[52] G. Baym, H. A. Bethe, and C. J. Pethick, *Neutron star matter*, Nuclear Physics A **175** (1971), no. 2 225 – 271.

[53] G. Baym, C. Pethick, and P. Sutherland, *The Ground State of Matter at High Densities: Equation of State and Stellar Models*, Astrophys. J.**170** (1971) 299.

[54] J. D. Walecka, *A Theory of highly condensed matter*, Annals Phys. **83** (1974) 491–529.

[55] J. Boguta and A. Bodmer, *Relativistic calculation of nuclear matter and the nuclear surface*, Nucl. Phys. **A292** (1977) 413.

[56] J. Boguta and H. Stöcker, *Systematics of nuclear matter properties in a non-linear relativistic field theory*, Phys. Lett. (1983) 289.

[57] G. A. Lalazissis, J. Konig, and P. Ring, *New parameterization for the Lagrangian density of relativistic mean field theory*, Phys. Rev. C**55** (1997) 540.

[58] N. K. Glendenning, *Neutron Stars Are Giant Hypernuclei?*, Astrophys. J. **293** (1985) 470–493.

[59] N. K. Glendenning and S. A. Moszkowski, *Reconciliation of neutron-star masses and binding of the Lambda in hypernuclei*, Physical Review Letters **67** (1991) 2414–1417.

[60] S. Typel and H. H. Wolter, *Relativistic mean field calculations with density-dependent meson-nucleon coupling*, Nucl.Phys.A **656** (1999) 331.

[61] A. Drago, A. Lavagno, G. Pagliara, and D. Pigato, *Early appearance of Δ isobars in neutron stars*, Phys. Rev. C**90** (2014) 065809.

[62] J. M. Lattimer and Y. Lim, *Constraining the symmetry parameters of the nuclear interaction*, Astrophys. J.**771** (2013) 51.

[63] K. Hebeler, J. M. Lattimer, C. J. Pethick, and A. Schwenk, *Equation of State and Neutron Star Properties Constrained by Nuclear Physics and Observation*, Astrophys. J.**773** (Aug., 2013) 11, [`arXiv:1303.4662`].

[64] P. Danielewicz and J. Lee, *Symmetry energy II: Isobaric analog states*, Nuclear Physics A **922** (2014) 1.

[65] J. M. Lattimer and A. W. Steiner, *Constraints on the symmetry energy using the mass-radius relation of neutron stars*, European Physics Journal A **50** (2014) 40.

[66] W. M. Spinella, *A Systematic Investigation of Exotic Matter In Neutron Stars*. PhD thesis, The Claremont Graduate University, 2017.

[67] T. Miyatsu, M. Cheoun, and K. Saito, *Equation of state for neutron stars in SU(3) flavor symmetry*, Phys. Rev. C**88** (2013) 015802.

[68] T. A. Rijken, M. M. Nagels, and Y. Yamamoto, *Baryon-baryon interactions*, Progress Theoretical Physics Supplements **185** (2010) 14.

[69] S. Typel, *Relativistic model for nuclear matter and atomic nuclei with momentum-dependent self-energies*, Phys.Rev.C **71** (2005) 064301.

[70] S. Typel, G. Röpke, T. Klähn, D. Blaschke, and H. H. Wolter, *Composition and thermodynamics of nuclear matter with light clusters*, Phys. Rev. C**81** (2010), no. 1 015803, [`arXiv:0908.2344`].

[71] A. W. Steiner, M. Hempel, and T. Fischer, *Core-collapse Supernova Equations of State Based on Neutron Star Observations*, Astrophys. J.**774** (2013) 17, [`arXiv:1207.2184`].

[72] S. Banik, M. Hempel, and D. Bandyopadhyay, *New Hyperon Equations of State for Supernovae and Neutron Stars in Density-dependent Hadron Field Theory*, Astrophysical Journal, Supplement **214** (2014) 22, [`arXiv:1404.6173`].

[73] A. Mishra and H. Mishra, *Color superconductivity and gapless modes in strange quark matter at finite temperatures*, Phys. Rev. D**71** (Apr., 2005) 074023, [`hep-ph/0412213`].

[74] D. G. Dumm, D. B. Blaschke, A. G. Grunfeld, and N. N. Scoccola, *Color neutrality effects in the phase diagram of the Polyakov–Nambu–Jona-Lasinio model*, Phys. Rev. D**78** (2008), no. 11 114021, [`arXiv:0807.1660`].

[75] S. Rößner, C. Ratti, and W. Weise, *Polyakov loop, diquarks, and the two-flavor phase diagram*, Phys. Rev. D**75** (2007), no. 3 034007, [`hep-ph/0609281`].

[76] R. Schaeffer, L. Zdunik, and P. Haensel, *Phase transitions in stellar cores. I - Equilibrium configurations*, Astron. Astrophys. **126** (1983) 121–145.

[77] R. C. Pereira, P. Costa, and C. Providência, *Two-solar-mass hybrid stars: A two model description using the Nambu-Jona-Lasinio quark model*, Phys. Rev. D**94** (Nov., 2016) 094001, [`arXiv:1610.0643`].

[78] S. Benic, D. Blaschke, D. E. Alvarez-Castillo, T. Fischer, and S. Typel, *A new quark-hadron hybrid equation of state for astrophysics - I. High-mass twin compact stars*, Astron. Astrophys. **577** (2015) A40, [`arXiv:1411.2856`].

[79] F. Cipolletta, C. Cherubini, S. Filippi, J. A. Rueda, and R. Ruffini, *Fast rotating neutron stars with realistic nuclear matter equation of state*, Phys. Rev. D**92** (July, 2015) 023007, [`arXiv:1506.0592`].

[80] J. R. Torres, F. Gulminelli, and D. P. Menezes, *Examination of strangeness instabilities and effects of strange meson couplings in dense strange hadronic matter and compact stars*, Phys. Rev. C**95** (Feb., 2017) 025201, [`arXiv:1608.0510`].

Table III. Properties of the compact stars arising from the hybrid EoS: GM1(L) plus 2SC+s (for $M_s^0 = 500$ MeV, $\Delta_s = 50$ MeV and $\eta_{qq} = 1.20$). We show the parameter values for the phase transition, $p_{\rm trans}/\varepsilon_{\rm trans}$ and $\Delta\varepsilon/\varepsilon_{\rm trans}$, varying the vector coupling constant η_v. The value $\langle c_{\rm QM}^2 \rangle$ is obtained by calculating the slope of the quark EoS through a linear fitting. We also give the mass and radius of the heaviest hadronic star ($M_{\rm trans}$ and $R_{\rm trans}$) and the mass and radius range (ΔM and ΔR) of the hybrid branch, calculated from the 2SC+s EoS and the CSS parametrization separately. For CSS we pick up the minimum or maximum of the speed of sound for quark matter and assume a constant $c_{\rm QM}^2$ to be of that value. The masses are expressed in $M_\odot$ and the radii in kilometers.

η_{qq}	η_v	$p_{\rm trans}/\varepsilon_{\rm trans}$	$\Delta\varepsilon/\varepsilon_{\rm trans}$	$\langle c_{\rm QM}^2 \rangle$	$M_{\rm trans}$	$R_{\rm trans}$	$\Delta M_{\rm 2SC+s}$	$\Delta M_{\rm CSS}$	$\Delta R_{\rm 2SC+s}$	$\Delta R_{\rm CSS}$
1.2	0.90	0.148	0.05	0.390	1.62	12.78	0.36	$(0.34, 0.71)$	-1.47	$(-1.28, -1.59)$
1.2	1.00	0.117	0.04	0.390	1.40	12.85	0.62	$(0.52, 1.07)$	-1.48	$(-1.09, -1.14)$

Table IV. Properties of the compact stars arising from the hybrid EoS: GM1(L) plus 2SC+s (for $M_s^0 = 600$ MeV). See caption of Table III for more information.

η_{qq}	η_v	$p_{\rm trans}/\varepsilon_{\rm trans}$	$\Delta\varepsilon/\varepsilon_{\rm trans}$	$\langle c_{\rm QM}^2 \rangle$	$M_{\rm trans}$	$R_{\rm trans}$	$\Delta M_{\rm 2SC+s}$	$\Delta M_{\rm CSS}$	$\Delta R_{\rm 2SC+s}$	$\Delta R_{\rm CSS}$
1.2	0.90	0.148	0.05	0.420	1.62	12.78	0.35	$(0.32, 0.58)$	-1.26	$(-1.22, -1.59)$
1.2	1.00	0.117	0.04	0.420	1.40	12.85	0.68	$(0.52, 0.95)$	-1.24	$(-1.04, -1.14)$

Table V. Properties of compact stars computed for the hybrid EoS DD2 plus 2SC+s (for $M_s^0 = 500$ MeV and $\Delta_s = 50$ MeV). We show parameter values for the phase transition, $p_{\rm trans}/\varepsilon_{\rm trans}$ and $\Delta\varepsilon/\varepsilon_{\rm trans}$, varying the vector coupling constant η_v and the diquark coupling constant η_{qq}. The value $\langle c_{\rm QM}^2 \rangle$ is obtained by calculating the slope of the quark EoS, through a linear fitting. We also give the mass and radius of the heaviest hadronic star ($M_{\rm trans}$ and $R_{\rm trans}$), the mass and radius range (ΔM and ΔR) of the hybrid branch, calculated from the 2SC+s EoS and the CSS parametrization separately. For CSS due to negligible variance in the speed of sound for 2SC+s quark matter we assume constant $c_{\rm QM}^2$ to be of the mean value $\langle c_{\rm QM}^2 \rangle$. The masses are expressed in $M_\odot$ and the radii in kilometers. See also Fig. 7 for mass-radius relations.

η_{qq}	η_v	$p_{\rm trans}/\varepsilon_{\rm trans}$	$\Delta\varepsilon/\varepsilon_{\rm trans}$	$\langle c_{\rm QM}^2 \rangle$	$M_{\rm trans}$	$R_{\rm trans}$	$\Delta M_{\rm 2SC+s}$	$\Delta M_{\rm CSS}$	$\Delta R_{\rm 2SC+s}$	$\Delta R_{\rm CSS}$
1.1	0.65	0.201	0.441	0.330	1.89	13.38	0.015	0.009	-0.27	-0.191
1.1	0.70	0.261	0.446	0.355	2.14	13.17	0.005	0.003	-0.03	-0.032
1.2	1.00	0.185	0.150	0.398	1.81	13.42	0.280	0.503	-1.33	-1.071